

## Friction modifiers effects on tribological behaviour of bainitic rail steels

Messaadi, Maha; Oomen, Matthijs; Kumar, Ankit

**DOI**

[10.1016/j.triboint.2019.105857](https://doi.org/10.1016/j.triboint.2019.105857)

**Publication date**

2019

**Document Version**

Accepted author manuscript

**Published in**

Tribology International

**Citation (APA)**

Messaadi, M., Oomen, M., & Kumar, A. (2019). Friction modifiers effects on tribological behaviour of bainitic rail steels. *Tribology International*, 140, Article 105857. <https://doi.org/10.1016/j.triboint.2019.105857>

**Important note**

To cite this publication, please use the final published version (if applicable).  
Please check the document version above.

**Copyright**

Other than for strictly personal use, it is not permitted to download, forward or distribute the text or part of it, without the consent of the author(s) and/or copyright holder(s), unless the work is under an open content license such as Creative Commons.

**Takedown policy**

Please contact us and provide details if you believe this document breaches copyrights.  
We will remove access to the work immediately and investigate your claim.

# Friction modifiers effects on tribological behaviour of bainitic rail Steels

Maha Messaadi<sup>a1</sup>, Matthijs Oomen<sup>b</sup>, Ankit Kumar<sup>c</sup>

<sup>a</sup>Section of Road and Railway Engineering, Faculty of Civil Engineering and Geosciences, Delft University of Technology, Stevinweg 1, 2628 CN, Delft, The Netherlands

<sup>b</sup>University of Twente, Laboratory of Surface Technology and Tribology, PO Box 217, 7500 AE, Enschede, The Netherlands

<sup>c</sup>Department of Materials Science and Engineering, Delft University of Technology, Delft, The Netherlands

Received Date Line (to be inserted by Production) (8 pt)

---

## Abstract

Bainitic steels are gaining popularity for application in the railway switches and crossing, thanks to their better rolling contact fatigue (RCF) and wear resistance. The rail degradation caused by RCF and wear could be also reduced by the use of friction modifiers (FM) through their ability to reduce the lateral load during wheel passage. This paper presents the microstructure and the mechanical properties of newly designed bainitic steel grades; B1400+ and Cr-B potential candidates for switches and turnouts railroad industry. It investigates their friction and wear performances using the HORIZONTAL twin DISK Machine. The tribological behavior is evaluated under dry and lubricated conditions in combination with three commercial friction modifiers. Results show a better wear resistance of Cr-B steel in case of abrasive mechanism that dominates the dry experiments. This work defines the efficiency of FM as a low and stable friction coefficient concomitant to a low wear rate. It appears that a good tribological performance is untimely linked to the chemical composition of the friction modifier. In case of lubricated contact, cross-sectioning of wear scars confirms the generation of interfacial layers. These layers have an impact on the wear mechanism and debris detachment susceptibilities of bainitic steels.

*Keywords: Rail grades, Friction modifier, Friction kinetics, Interfacial layer, Wear mechanisms.*

---

© 2019 Manuscript version made available under CC-BY-NC-ND 4.0 license  
<https://creativecommons.org/licenses/by-nc-nd/4.0/>

---

\* Corresponding author: E-mail address: [M.Messaadi@tudelft.nl](mailto:M.Messaadi@tudelft.nl)

## 1. Introduction

Wheel-rail contact is a tiny area; roughly  $1 \text{ cm}^2$  [1], where a complex tribo-system operates with respect to the mechanical loading, materials and the environment. Generally, this zone joins the wheel steel and rail steel as continuous patch belongings under combined rolling-sliding motion in straight tracks [2]. However, when trains pass over switches and crossings, the wheel-rail contact becomes intermittent holding often under dynamic impact loads due to the track discontinuities at turnouts [3]. In both configurations, an excessive loading; high train speed, high axle force, high creepage percentage, would damage wheel and rail steel surfaces mainly by two major factors; wear and rolling contact fatigue (RCF) [4,5]. The rolling contact fatigue (RCF) appears as cracks that may be initiated in the worn surface or the subsurface and propagates by the action of the repeated wheel-rail contact.

The increasing damage statistics in railway switches and crossing requires the use of high strength steels with increased wear and RCF resistance. The introduction of bainitic steel, with improved mechanical properties than conventional pearlitic steels, can suppress the damage in railway switches and crossings. Additionally, the correct use of friction modifiers in combination with suitable steel grade can further enhance the component lifetime. This can also lead to the reduction of maintenance costs to the rail industries and also ensure safety. Recent development of some bainitic grades such as low carbon carbide free bainitic steels showed improved mechanical properties and RCF resistance than the conventional pearlite grades [6][8][1-3]. However, these developments still show insufficient wear resistance specially for use in rail crossings applications [6].

The wear resistance is considered as the ability of surfaces to loss progressively or displace their material by the action of relative motion between surfaces or a surface and another substance [9]. The gradual rail material losses occur usually by an adhesive or abrasive mechanism depending on the contact nature and loading history; dry or lubricated [10]. Lewis et al. [11] discussed the rail wear regimes. They considered that it was imprecise to identify the wear mechanism causing transitions from one regime to another. Nevertheless, they established a map indicating an explicit relationship between wear rate and the sliding velocity. In other words, the wear kinetics depend on the micro-slips resulting from severe friction between the wheel and rail. The wear reduction in wheel and rail is possible primarily through two manners:

- Improving the wear and RCF resistance by modifying the microstructure of both wheel and rail steels. This is achievable via material processing as example heat treatments. The steel microstructure influences the mechanical properties such as the hardness, toughness and fatigue strength.
- Reducing the wheel-rail traction forces; sliding velocities, by the application of friction modifiers (FM) in the railhead. The cyclic loading, in presence of FMs, forms an interfacial layer which would reduce the friction through the suspension constituents [12].

Recently, Hardwick et al. [13] suggested a classification of friction management products regarding their influence on promoting RCF damage. The ranking list compares between FMs products regarding their carrier; water, lubricant and oil. They inferred that the use of the oil friction modifier on the top of rail would reduce the wear between 0.06-72 percent within slight cracks interactions. The present research focuses on the efficiency of commercial FMs to protect rail bainitic grades against rail wear. The originality of this work consists mainly in three aspects:

- The study of microstructure and mechanical properties of newly designed bainitic steels; B1400+ and Cr-B. These alloys are currently used in Germany for crossings applications, despite the rare studies that are available on their material characterization and wear behaviour.
- The evaluation of the tribological performances of the designed bainitic grades in the presence of FMs.
- The study of the interlayer, or the third body, induced on the worn surfaces with respect to the FMs composition. This thin interlayer generation kinetics and its role in surface protection against different wear mechanisms.

The structure of this work is as follows. Section 2 presents the bainitic and pearlitic grades detailing their microstructures and mechanical properties. Furthermore, the morphologies and chemical composition of the oil suspensions formulating the commercial friction modifiers are highlighted. This section ends with the establishment of the experimental conditions in connection with a representative wheel-rail contact. Section 3 presents frictional and wear behaviours of the various experiments. Section 4 discusses these results in relation to interlayers generated on contacting surfaces. Section 5 closes with conclusions.

## 2. Experimental details

### 2.1. Materials

#### 2.1.1 Bainitic steels

Table 1 shows the chemical composition of conventional pearlitic grade; R260, and two selected steels B1400+ and Cr-B. Both bainitic steels are low-carbon alloys. The carbon content is almost the same 0.36 wt%. The convenience of the use of a low carbon concentration is that the steel can be easily welded principally in switches and crossings infrastructures [14]. The specimens of B1400+ and Cr-B were supplied by Voestalpine and DB Bahn, Germany. Samples are cut in the form of discs and heat treated according to the cycle presented in Fig.1. Indeed, steels as received are not immediately appropriate to be used as rail and/or switches components. This is due to the fair amount of unwanted phases in their microstructures namely the residual austenite and martensite. The isothermal bainitic transformation aims to minimize these phases.

Table 1 Composition of the conventional pearlitic rail steel (R260) and selected steels (B1400+ and Cr-B) for bainitic transformation.

Steel Grade	C wt.%	Cr wt.%	Mn wt.%	Si wt.%	V wt.%	Mo wt.%	S wt.%	Cu wt.%	Al wt.%	P wt.%	Ni wt.%
R260	0.67	0.1	1.5	0.21	-	-	-	-	0.002	0.003	-
B1400+	0.363	1.146	0.934	0.694	0.095	0.713	0.0009	0.242	-	-	0.223
CrB	0.367	2.722	0.726	0.595	0.109	0.3	0.0008	0.05	0.0069	0.0059	0.059

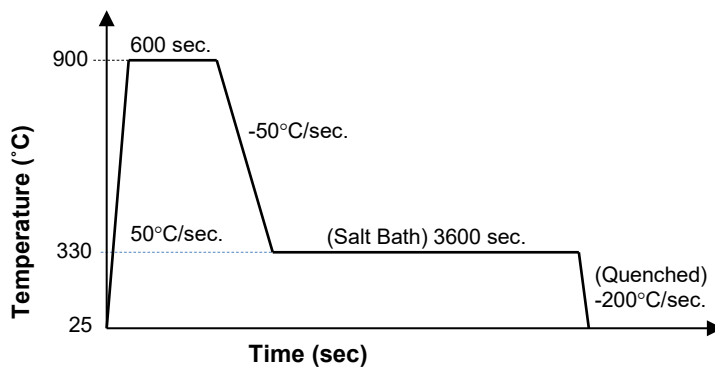


Fig. 1. Schema showing the used heat treatment for isothermal bainitic transformation for B1400+ and Cr-B steel.

Fig.1 describes the heat treatment scheme used for the isothermal bainitic transformation of both steel disks. The disks were first heated to full austenitization zone at 900 °C for 600 seconds. Afterwards, the disks were transferred to constant temperature salt bath maintained at 330 °C. To ensure an appropriate isothermal bainitic transformation, the disks were kept in the salt bath for 3600 seconds and then quenched in oil. Resultant microstructures are studied in paragraph 3.1. The amount of the blocky retained austenite is also evaluated by presentation of the EBSD IQ + austenite phase map.

### 2.1.2 Friction modifiers (FMs)

The studied friction modifier lubricants are oil-based carrier with dispersed solid particles. Various products are available in railway commerce [15–17]. Oomen et al. [18] examined the chemical and morphological characteristics of three commercial FMs nominated in this work by FM-C, FM-S and FM-A. Lubricants properties are summarised as follows:

- The three FM suspensions have comparable dynamic viscosity : 0,033- 0,042 Pa.s<sup>-1</sup> at 40 °C,
- Synthetic ester oil as a common carrier,
- Volume fraction of solid particles varies between 0.25-0.55 [18].

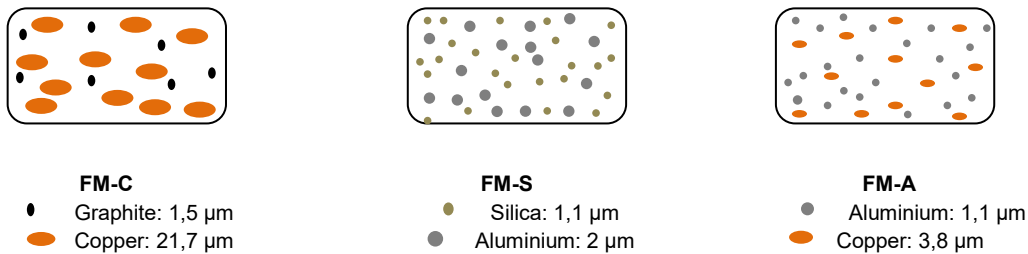


Fig. 2. Qualitative description of chemical nature of solid particles constituents of the three FMs, values from [18].

Fig.2 compares qualitatively the chemical nature of solid particles constituents of different suspensions. It shows that FM-C contains a relatively bigger copper particles size comparatively to other suspensions. Large copper particles are probably flattened. Additionally, it contains a solid lubricant that is graphite. FM-S includes also a non-metallic element; the silica. Besides, FM-A suspension comprises only metallic particles; copper and aluminium with comparable sizes.

## 2.2 Tribological tests

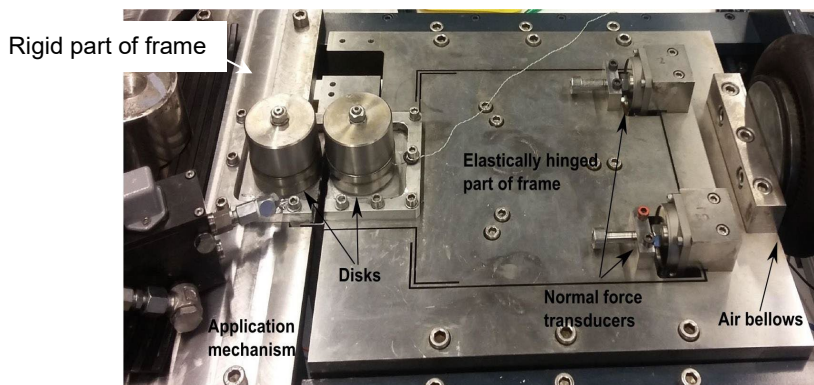


Fig. 3. Image of HODIM set-up.

Rolling-sliding experiments were carried out using the HORIZONTAL twin Disk Machine (HODIM) at the University of Twente, see Fig. 3. The working principle of the tribometre is based on the difference of rotation load and speed between an elastic and rigid parts of a set-up. On the right, a disk and a motor are mounted on a frame supported by a set of leaf springs. When the air bellows provides the normal load. It is transmitted to the right side disc through hinges having a limited stiffness in torsional direction compared to the normal. This allows a free rotation of the motor. The difference in the normal loads measured in the force transducers, which in turn gives a measure for the friction present in the disk-disk contact. This working principle guaranties the elimination of the undesirable internal friction of the motor and gear assembly. Further details concerning the tribometer characteristics are available in the work of Oomen et. al. [18].

This study investigates the friction and wear performances of newly developed bainitic steels in the presence of FMs. Similar studies are rarely available in the literature despite of the growing interest in bainitic alloys. Tribology test consists on the use of reference material, R260 steel grade. Each pair, *i.e.* B1400+/R260 and CrB/R260, is tested firstly under dry sliding, and secondly under lubricated conditions.

After the heat treatment of bainitic steels, discs are machined to acquire a conic geometry in the aim to create an elliptical contact path during tribology test. Discs made from same batch of R260 are also machined. The expected running pattern is properly polished. The specimens of bainitic steels are polished using 320 and 1000 grit SiC papers

after mounting the discs on the lath machine. However, the pearlitic steels are not polished and used directly after the machining. The time of polishing and the rotational speed of the lath machine for both the SiC papers are kept constant to achieve uniform surface finish in the bainitic specimens.

The twin Disc tribometer parameters are adjusted to reproduce approximately wheel-rail conditions:

- Contact pressure varying around 0.5 - 0.55 GPa,
- A combined rolling and sliding motion at two slip ratios:
  - 0.5% slip during normal de-acceleration of wheel-rail,
  - 11% slip comparable to the emergency braking sliding condition.
- Periodical application of 20  $\mu$ L of FMs, which is similar to the industrial practice. A new dose of FM was applied to the contact when the friction level reaches 0.3.

During experiments, the friction coefficient kinetic (called also traction) is recorded instantaneously making possible the examination of FMs efficiency. The number of repetitions is two due to the limited amount of disks available for testing. Therefore, the friction response under progressive lubricated conditions is examined; a fully flooded condition exists just after the application of the suspension and a hydrodynamic lubrication regime occurs. This layer rapidly decreases in thickness, leading to starved lubrication conditions with a thin layer of FM. The efficiency of the FM is defined as the suspension ability to:

- hold a stable friction coefficient between 0.2 to 0.3,
- within a minimal numbers of suspension application,
- and leading to relatively low wear volume in bainitic and pearlitic steels.

### **2.3 Analytical tools**

The microstructure of B1400+ and Cr-B steel is characterized using Secondary Electron (SE) imaging and Electron BackScatter Diffraction (EBSD) technique in a JEOL JSM 6500F scanning electron microscope. An accelerating voltage of 15 KV, working distance of 18 mm and step size of 50 nm in hexagonal scan grid is used for EBSD scanning. Orientation Image Microscopy (OIM) software (TSL-OIM) is employed to analyze the EBSD data.



Mechanical properties of hear studied steels are determined using standard tensile testing on ASTM sub sized cylindrical dog bone specimens (gauge length = 25 mm and gauge diameter = 8mm ) with a constant crosshead speed of 1mm/min on Instron 2200 machine.

At the end of tribology test, the wear volumes, by the calculation of the mass loss, are evaluated using a confocal microscope which allows to access to the surface morphology. Concerning the wear measurements, all disks are marked to be able to measure the same point before and after the tests. Before microscopic measurements, disks are immersed for 5 minutes in beaker with isopropanol solvent in an ultrasonic bath.

### 3. Results and discussion

#### 3.1 Microstructure and mechanical properties of bainitic steels

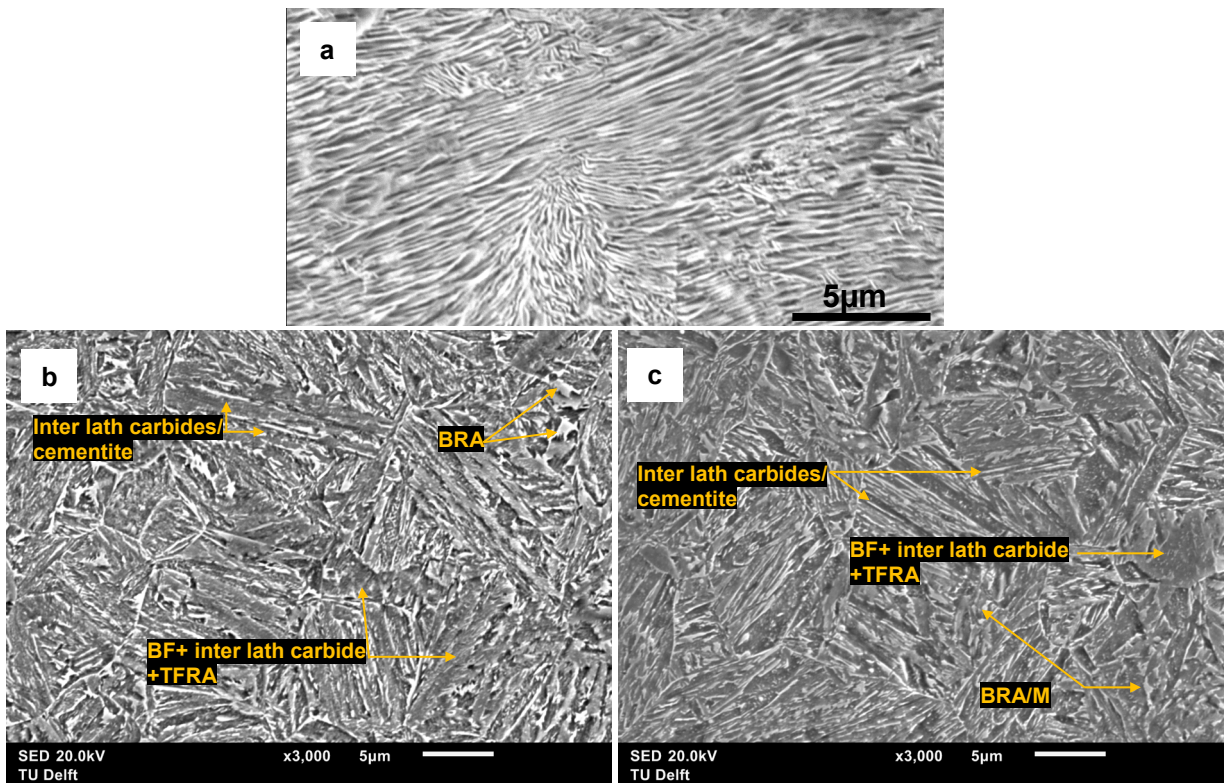


Fig. 4. SEM of microstructures of bainitic and pearlitic steel; a- pearlitic steel R260,b-bainitic steel B1400+ and c- bainitic steel CrB.

The mechanical properties such as strength, hardness and toughness of steels depend strongly on their microstructure. Thus, it is essential to characterize the microstructure and mechanical properties of the studied materials. Fig.4 compares microstructures of bainitic steels to conventional pearlitic steels.

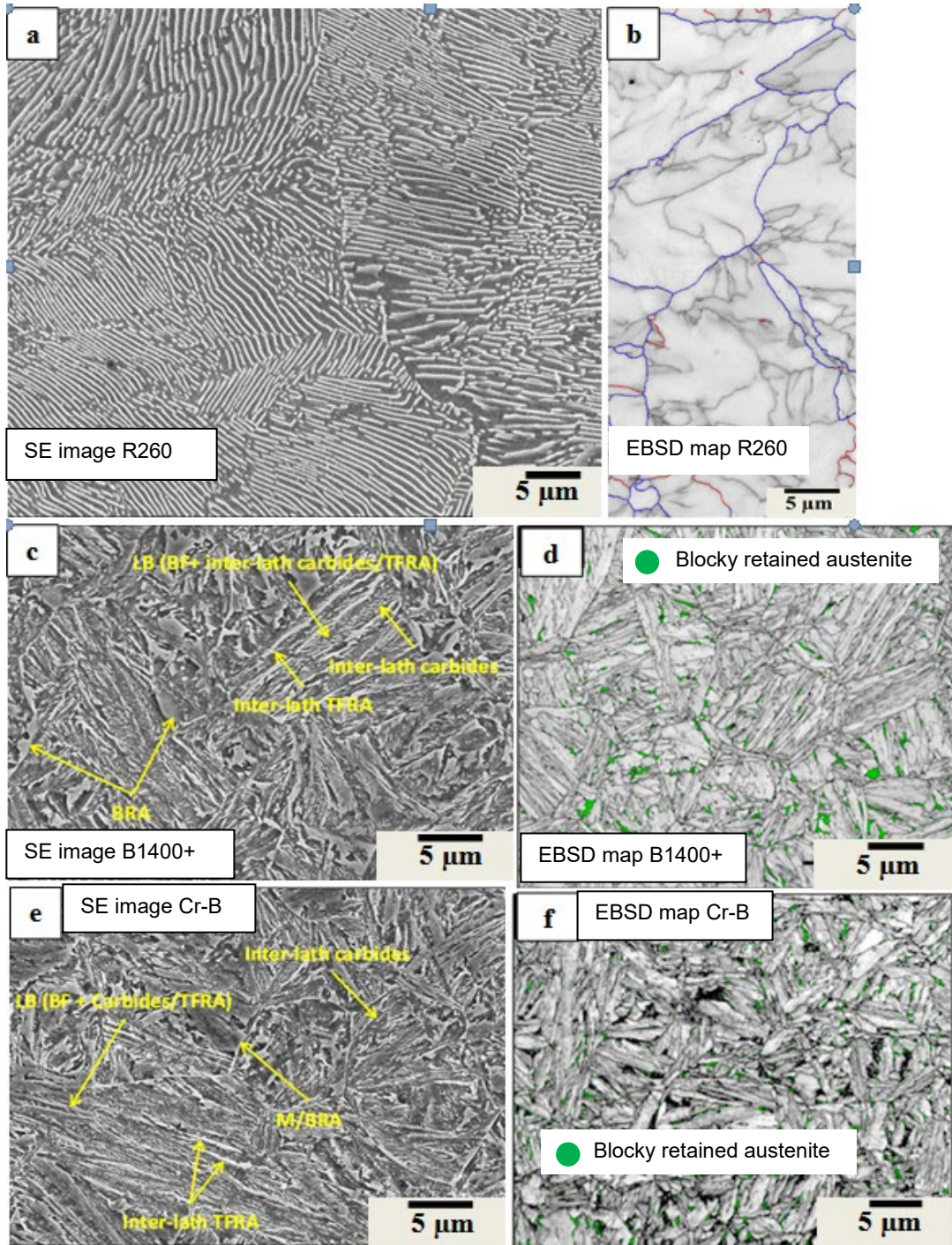


Fig. 5. Secondary electron (SE) images and image quality (IQ) electron backscatter diffraction (EBSD) maps showing the microstructure of (a,b) R260 pearlitic steel (c,d) B1400+ bainitic steel; (e,f) Cr-B bainitic steel; (a,c,e) SE images, (b,d,f) EBSD IQ + austenite phase maps (blocky austenite in green).

Fig.4a presents the microstructure of R260 steel. It is a full pearlitic microstructure where cementite lath (white) are sandwiched between ferrite laths (grey). The inter-lamellar spacing in the pearlitic microstructure ranges in between 200-250 nm. An image quality (IQ) EBSD map is proposed in Fig.5a for R260 to evaluate pearlitic colonies size. Results indicate large range of about 15 to 25  $\mu\text{m}$ .

The bainitic steels, Fig.4b-c, show finer microstructures than R260 pearlitic steel. The grain refinement is achieved due to the low isothermal temperature (330 °C) during bainitic transformation, as shown in Fig.1. Fig. 4b and c present the secondary electron (SE) image showing complex microstructures of B1400 + and CrB steels, containing multiple phases:

- bainitic ferrite (BF),
- thin film retained austenite (TFRA),
- blocky retained austenite (BRA),
- inter lath carbides/cementite,
- martensite (M) for CrB steel.

The EBSD IQ + austenite phase map of B1400 + steels are also used to identify the blocky retained austenite, see Fig.5d and f. The result shows that B1400 + microstructure contains  $\approx 3.5\%$  of retained austenite blocks. Using same analytic technique, the Cr-B microstructure shows  $\approx 3\%$  of retained austenite blocks.

Table 2 Mechanical properties of studied rail grades i.e. R260, B1400+ and Cr-B steels.

Steel	Yield strength (MPa)	Ultimate strength (MPa)	Engineering fracture strain (%)	Hardness Hv <sub>0.1</sub>
R260	600±11	880±15	12±0.9	270±15
B1400+	1260±13	1678±14	8±1	533±8
CrB	1229±13	1657±15	10±0.7	537±7

Table 2 presents the mechanical properties of tested steels; pearlitic grade R260 and the bainitic steels B1400+, and CrB. It is obvious that bainitic steels have higher hardness, yield, and ultimate strength compared to the pearlitic grade.

### 3.2 Friction and wear results

This section distinguishes between the dry and lubricated conditions as a function of sliding ratio. Friction coefficient evolution and mass loss of both bainitic grades are compared. The purpose is to understand the tribological behavior of each rubbing system.

#### 3.2.1 Dry conditions

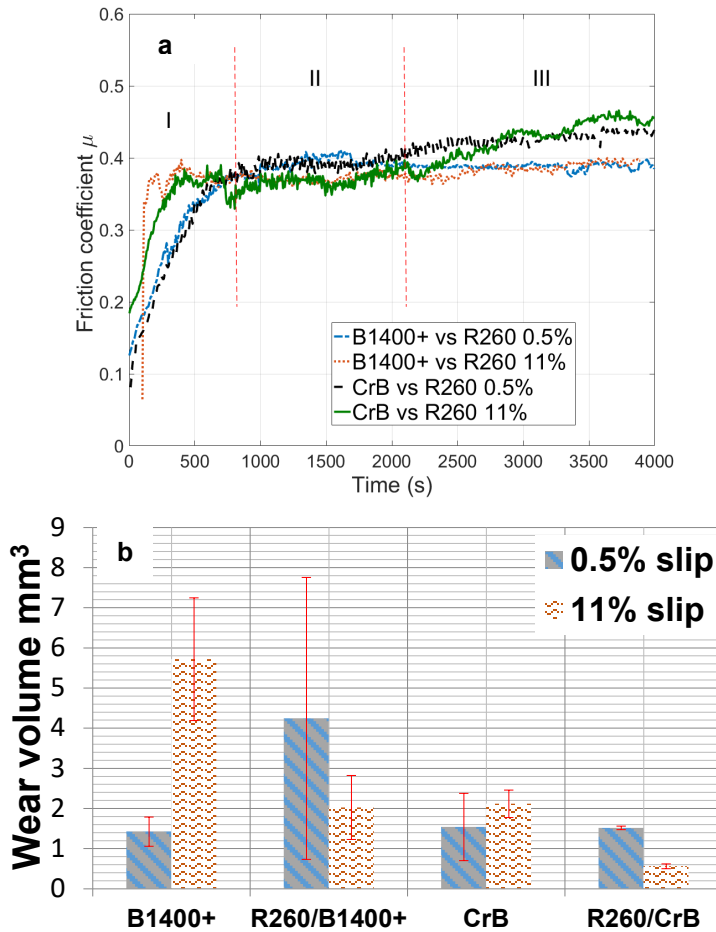


Fig. 6. Comparisons of friction behaviour (a) and wear volume (b) of B1400+/R260 and CrB/R260 materials in a dry condition as a function of % slip.

Fig.6 highlights the friction coefficient evolution and the induced wear volumes in bainitic and pearlitic steels. It shows the influence of the sliding ratios. Fig.6a presents the progress of the friction during 1h and 10 min of rolling-sliding experiment. It indicates three main stages:

- Stage I: 0- 800 s, the friction increases progressively due to surfaces accommodation. At this stage, the effect of slip ratio is visible; high slip ratio leads to shorter time to reach stable friction level.
- Stage II: 700 s – 2100 s, a steady friction region at comparable friction level 0.36 at 11 % and 0.39 at 0.5% regardless the rubbing pair,
- Stage III: 2100 s – end of test, this stage depicts different friction kinetics. B1400+/R260 holds a stable friction disregarding the slip ratio until the end of the experiment. Contrary, the friction evolution of CrB/R260 increases again without reaching a stable value at the end of the experiment. This stage is determined not only by taking into account the CrB/R260 system but also B1400+/R260. Even the friction slope starts his increase earlier within CrB, it still at comparable level to B1400+/R260. The boundary of the third stage starts when the friction of CrB/R2600 clearly higher than B1400+/R260.

Fig.6b presents the measured mass loss in bainitic and pearlitic discs at the end of the rolling-sliding experiment for both slip ratios. It seems that at 0.5% slip ratio, wear volumes of B1400+ and CrB are comparable. But the pearlite steel rubbing against B1400+ loses more material compared to that rubbed against CrB steel. The large variation of the error bar obtained within R260 material is attributed to the developpemt of a small corrugation marks in B1400+ disc leading to an acceleration of wear. The duplication of this test without the generation of corrugation leads to the decrease of wear volume but still higher than R260 material rubbing against CrB.

Moreover, at 11% of slip ratio, wear volume of bainitic steels increases when it decreases for pearlitic. Fig.6b shows that the mass loss susceptibility of B1400+/R260 is relatively higher than CrB/R260. To better understand the tribological reponse obtained in dry condition for each system (B1400+/R260, CrB/R260), it is essential to examine the involved wear mechanism.

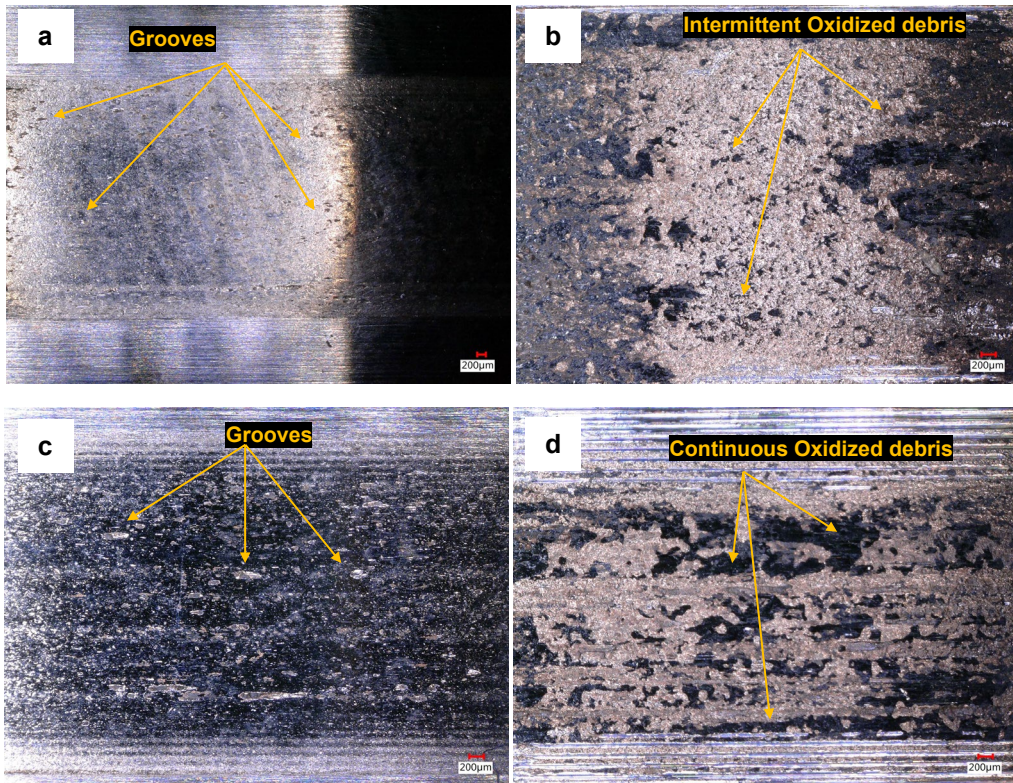


Fig. 7. Wear tracks observations after 11% of sliding ratio in dry condition, a-worn surface of B1400+ disc, b- worn surface on R260 disc rolling against B1400+, c- worn surface of CrB disc, d- worn surface on R260 disc rolling against CrB.

Fig. 7 presents optical observation of wear cicatrices induced in bainitic and pearlitic steels at 11% of slip ratio, Fig. 7a-b describes B1400+/ R260 system, and Fig. 7c-d presents CrB/R260 system. All worn surfaces show the presence of grooves and pitted surface indicating a severe abrasion. In case of pearlitic steels, it seems that the disc rubbing against B1400+, Fig. 7b, has larger contact patch leading to more material delamination. Besides, the surface of R260 rubbing against CrB is covered by oxidized debris trapped in the contact pattern contrary to R260 rubbed against B1400+.

With regard to friction coefficient evolution concomitant to the induced wear volume, the B1400+/ R260 system involves severe abrasion process. Detached debris from R260 surface are ejected continuously outside the contact area. Raw metallic surface is exposed to the material deletion. This appears as a steady friction coefficient. At low slip ratio, 0.5 %, abrasion is accentuated in pearlitic steel opposite to high slip ration where bainite steel generates probably more debris. Detached materials, even from pearlitic and/or baintic steels, are exposed to oxidation, see

intermittent oxidized debris in Fig.7b. Likely, as they are not eliminated from the contact area, they agglomerate as flocky portions at the surface of R260 disc leading to the relative decrease of wear volume.

Concerning CrB/R260 system, it shows better abrasion resistance. However, the increase of the friction coefficient could indicate a change of the wear processes. Generated debris at friction stage II are tarped in the contact area and caused an oxidized bed producing a competition between abrasive and transfer wear processes. As a consequence, the concomitance of abrasive and transfer mechanisms lead to an increase of the friction in stage III.

According to literature, the abrasion resistance could be related to the steel microstructure. Xu et al.[19] attempted to define a desired abrasion resistant microstructure. They explained that a dual phase material; Ferrite + Martensite would exhibit a better resistance compared to steel with a fully bainitic and/or pearlitic microstructure. Moreover, they delineate that the high hardness is not always required to reduce the wear. This finding fits with our results where the hardest steel, bainitic steel, generated an important mass loss compared to pearlitic steel. Xu et al.[19] expounded that the microstructure refinement could lead to the drop of the abrasion resistance. This result explains also that the wear volume rise obtained at 11% of slip. In addition, Dayot et al. [20] evaluated the capacity of bainitic and pearlitic steel to particle detachments. They argued a slight improvement of bainitic grades compared pearlite.

### **3.2.2 Friction and wear under lubricated conditions**

Under lubricated contact, the friction is controlled by the application of FM suspensions. During the running test, the first 400 seconds of each test is a dry running-in period, after that, around 20  $\mu$ L of FMs are consecutively added, when friction reaches 0.3, to keep a low friction level. The addition of FM suspensions leads to a drop of the friction coefficient. This sequence still ongoing until the generation of an interfacial layer that can inhibit the increase of the friction.

#### **3.2.2.1 Results of 0.5% slip**

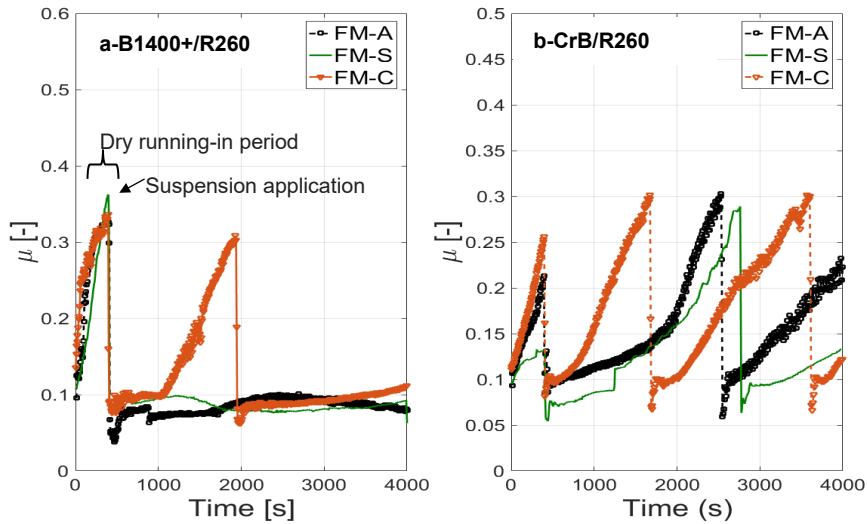


Fig. 8. Friction coefficient evolution as a function of lubricants at 0.5% of slip ratio, a- B1400+/ R260, b-CrB/R260.

Fig.8 compares friction responses in presence of the three FMs at 0.5% of slip ratio. Referring to Fig.8a, the friction between B1400+ and R260 discs increases quickly in dry period. Once the FM suspensions added, the friction drops immediately. Friction coefficient in presence of FM-A and FM-S suspensions keep lower level than 0.1 until the end of the experiment. Contrary to FM-C suspension, the friction coefficient increases after 16 min that required a new suspension dose application. Fig.8b displays the friction coefficient response of CrB/R260. It shows a triangular evolution indicating the successive increase and decrease of friction after suspension applications. Along the testing period, friction in presence of FM-C required 3 doses to ensure a lower coefficient values,  $< 0.3$ , compared to 2 doses in case of FM-A and FM-S. This confirms the advantageous lubrication performances of FM-A and FM-S compared to FM-C with both bainitic steels.

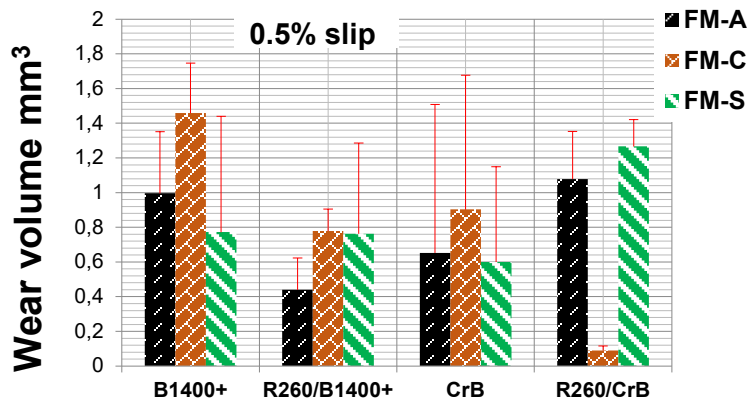


Fig. 9. Wear volumes of B1400+/R260 and CrB/R260 materials as a function of FMs at 0.5% of slip ratio.



Fig.9 summarizes the induced wear volumes at the end of lubricated rolling-sliding tests at 0.5% of slip ration. The graph points out that bainitic steels undergo highest damage in presence of FM-C suspension. Besides, FM-S suspensions give rise to wear in pearlitic steels. FM-A suspension generated acceptable wear on bainitic and pearlitic discs relatively to the other suspensions.

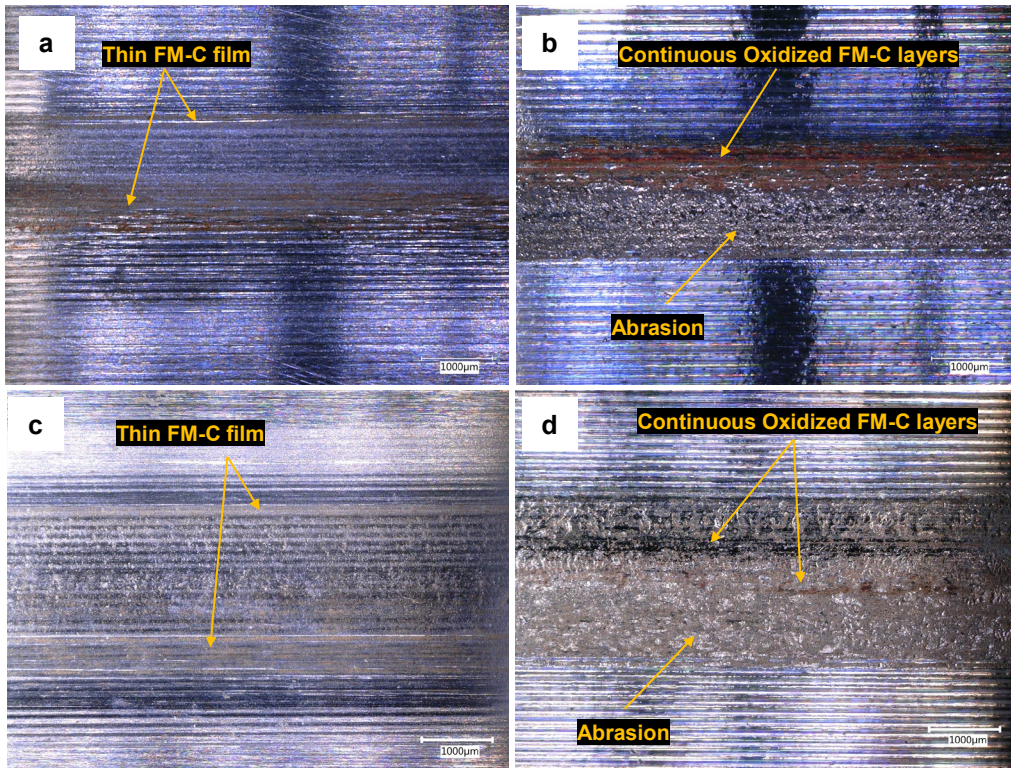


Fig. 10. Wear tracks observations after 0.5% of slip ratio in presence of FM-C suspension, a-worn surface of B1400+ disc, b- worn surface on R260 disc rolling against B1400+, c- worn surface of CrB disc, d- worn surface on R260 disc rolling against CrB.

Apropos of wear mechanisms, Fig.10 presents an overview of wear tracks induced in bainitic and pearlitic grades in presence of FM-C suspensions. The pearlitic discs in Fig.10b and d develop an abrasive contact patch, which are covered by oxidized and continuous thickness. Thinner and intermittent films appear to be generated in bainitic surfaces in Fig.10a and c. Solid particles of the FM are entrapped in the surface roughness. R260 worn surfaces manifest an accumulation of particles located in the upper contact edge. The abrasive process is relatively limited in bainitic steels that may be explained by the dominance of chemical and adhesive mechanisms. Samples in Fig.10a and

c are transversally sectioned in the aim to check the development of third body layers. Results will be discussed in paragraph 3.2.2.3.

### 3.2.2.2 Results of 11% slip

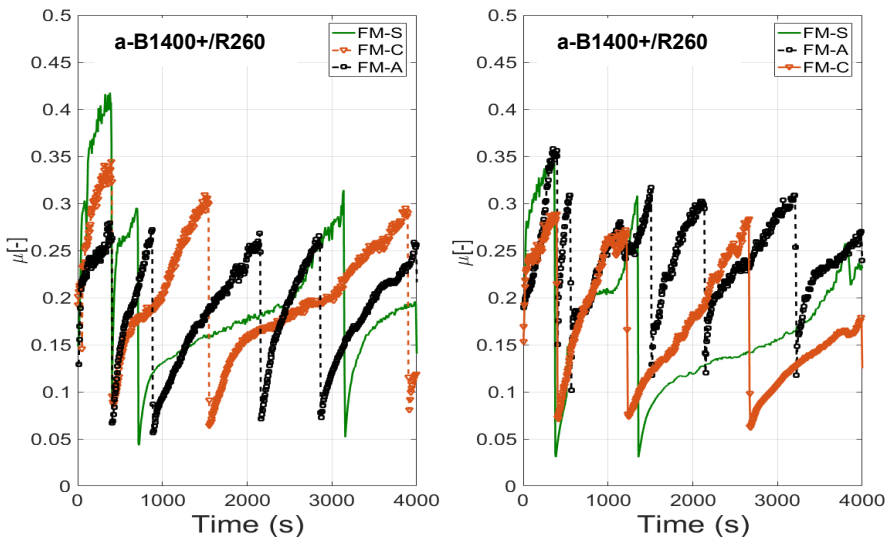


Fig. 11. Friction coefficient evolution as a function of lubricants, a- B1400+/ R260, b-CrB/R260.

The increase of the slip ration influences the consumption of FMs particle layer formed in the contact interface. This is clear in Fig.11, it shows more frequent suspension applications compared to the case of 0.5% slip ratio. In Fig. 11a, the application of suspensions after the dry running in period reduces the friction for a lapse of time, then it increases again following a distinguishable triangular shape. After the second suspension application, the friction increase kinetic is slowed down especially in case of FM-S suspension with the both tribo-systems, in Fig. 11a and b. The ascendant friction slop describes three stages:

- A rapid increase from 0.08 to 0.13,
- A continuous and slow friction increase from 0.13 to 0.2,
- A rapid increase from 0.2 to 0.3,

This behaviour is non-identical to FM-A and FM-C. Indeed, friction in presence of FM-A suspension looks similar to FM-S. However, the third stage is absent which means that the friction increases continuously from 0.18 to 0.3 without any slop changes. Concerning FM-C suspension, the friction preserves a progressive slop, no ascendant friction slop changes. The various friction behaviours confirm that the kinetic of inter-layers film construction is

untimely linked to tribo-system; the suspension composition, suspension particles rheology, wear debris detached from steel matrix, and the chemical affinities of metallic surfaces.

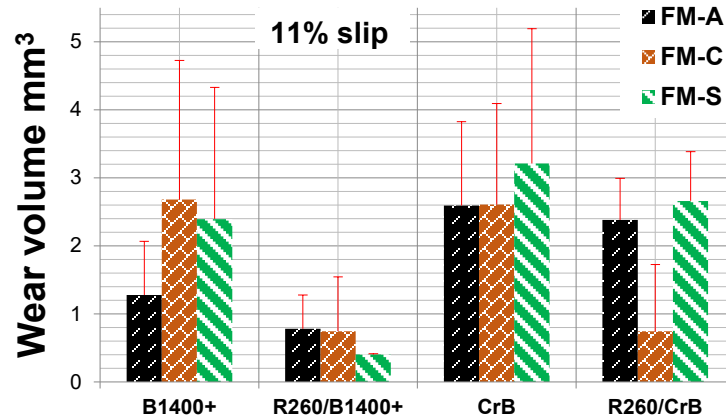


Fig. 12. Wear volumes of B1400+/R260 and CrB/R260 materials as a function FMs at 11% of slip ratio.

The different friction kinetics is dependent on the formation of the third body film and its adhesion on disc surfaces. The presence of this film also affects the wear rate and mechanisms. Histograms in Fig.12 present wear volumes obtained at the end of the rolling-sliding test at 11% of slip ratio and in presence of the various commercial FMs.

Generally, results show pearlitic steels wear less than the bainitic. This is in agreement with wear results obtained at 0.5% slip ratio. In addition, B1400+ disc undergoes the highest wear in presence of FM-C suspension, similar finding to 0.5% slip ratio. However, FM-S suspension induces relatively higher wear in CrB steel contrary to the 0.5% slip. At high slip ratio, the wear induced in CrB/R260 system is higher than in B1400+/ R260 that is a disparate result than the dry condition.

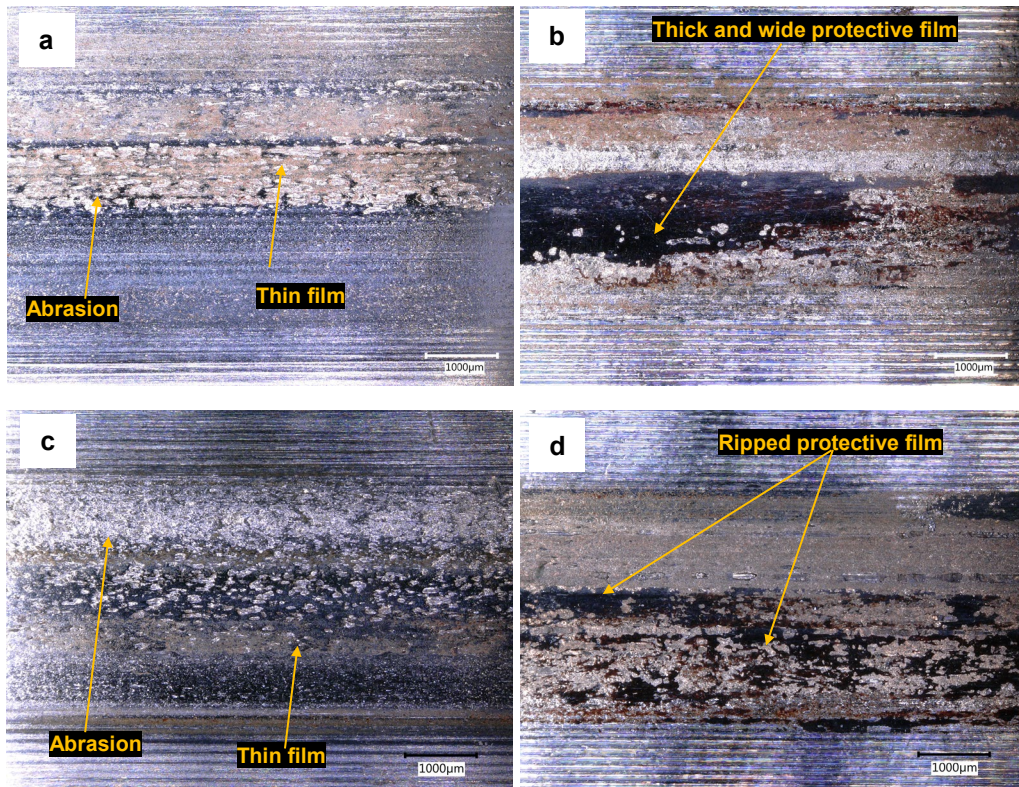


Fig. 13. Wear tracks observations after 11% of slip ratio (a-b) B1400+/R260 in presence of FM-C and (c-d) CrB/R260 in presence of FM-S, a- worn surface of B1400+ disc, b- worn surface on R260 disc rolling against B1400+, c- worn surface of CrB disc, d- worn surface on R260 disc rolling against CrB.

Fig.13 presents worn surfaces of B1400+ and CrB steels and their counter bodies at the end of experiments leading to the highest wear in bainitic grades. It shows that abrasive wear is developed in all surfaces. Furthermore, pearlitic surfaces present remarkable presence of solid particle films compared to bainitic, in Fig. 13b and d. Based on the optical observation, it is possible to distinguish between the third body film qualities. In case of B1400+/R260 system, FM-C generates thick film, which covers large contact zone, and adherent to R260 surface. In the other hand, FM-S induced a ripped film.

### 3.2.2.3 Efficiency of FMs

With reference to literature, several research teams investigate FM performances having various purpose such as the understanding of the influence of FM on corrugation, RCF, noise generation, and enhancing the adhesion. The multiple objectives lead to a confusing definition of the FM efficiency. That is why, it is important to clarify this

meaning. In fact, Oomen et. al.[18] explained the benefits to ensure a moderate friction coefficient between 0.2 to 0.3. This may be achievable in the case that FM suspension generates a stable third body at the interface. His quality depends on the suspension rheology during the tribology test. To point out clearly the generation of the third body, a cross-sectioning is performed exclusively in bainitic steels rubbing in presence of FM-C suspension at 5% of slip ratio. Indeed, this suspension contains the largest size of the copper particles, see paragraph 2.1.2. That means it would be possible to identify and characterize the third body using accessible equipment such as the SEM and EDS. Besides, for 11 % of slip ratio, Fig13 a and b show that the third body is located on the top surface of the pearlite steel which could be not relevant for the study.

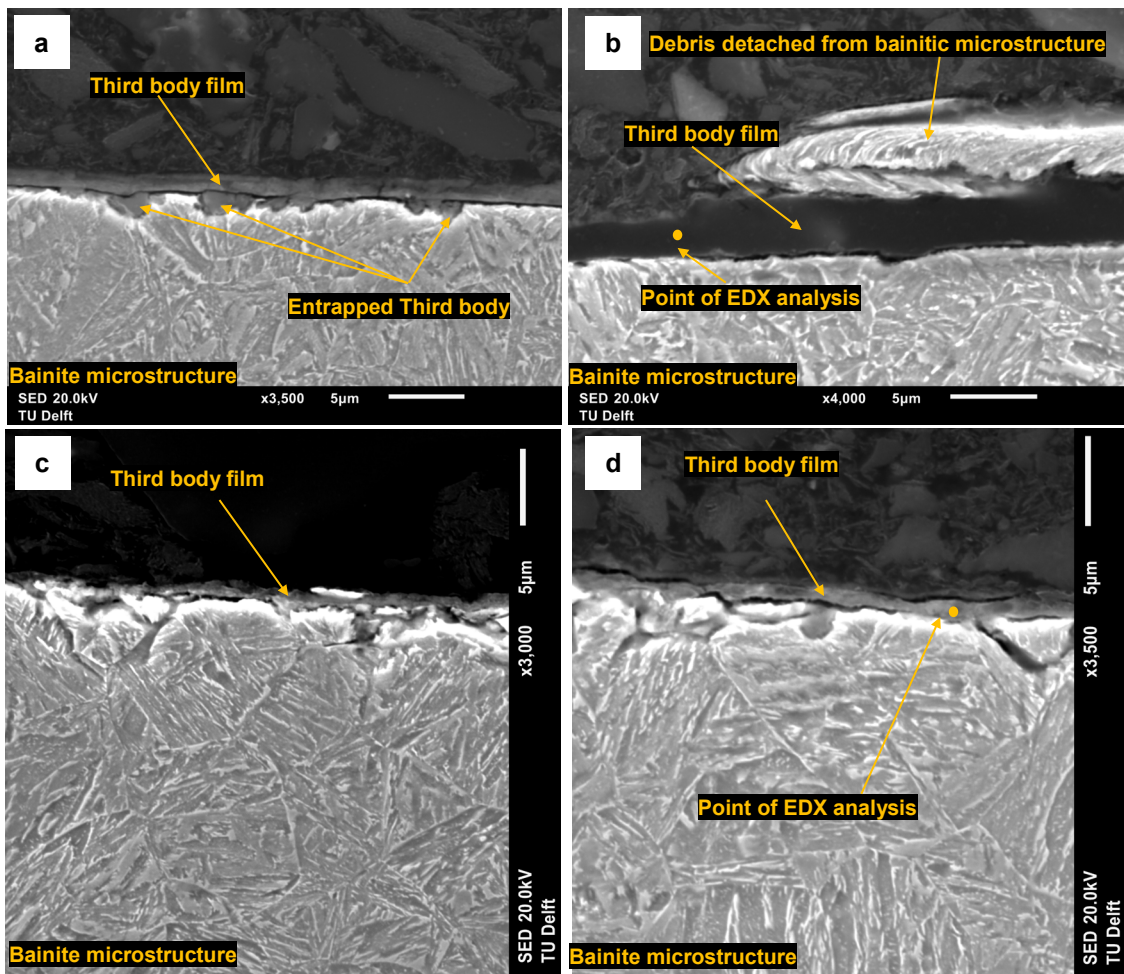


Fig. 14. SEM images of transversally cross-sectioned B1400+ and CrB samples after rolling sliding test in presence of FM-C suspension at 0.5% of slip ratio, a-b B1400+, c-d CrB.

Fig.14 illustrates the formation of third body layers in the top surface of bainitic steels at 0.5% of slip ratio. Fig.14a and b show cross-sections performed in disc of B1400+ steel, the worn surface is presented previously in Fig.10a. The thickness of these layers varies between 1.7 to 3.5  $\mu\text{m}$ . Fig.14a reveals that the third body is also entrapped in the surface roughness. On the other hand, Fig.14c and d present thinner layers developed at the surface of CrB steel under similar contact conditions. His thickness is around 1.2  $\mu\text{m}$  in Fig.12d.

It is important to remind that FM-C suspension contains principally an elongated copper particles and smaller graphite. Due to their size, coppers particles can hardly be trapped in surface roughness; most likely they are rejected outside of the contact area. Fig.10b shows a clear accumulation of copper in the upper contact edge. For a deeper understanding of third bodies' generation, EDS analysis are performed in points indicated in Fig.14b and d.

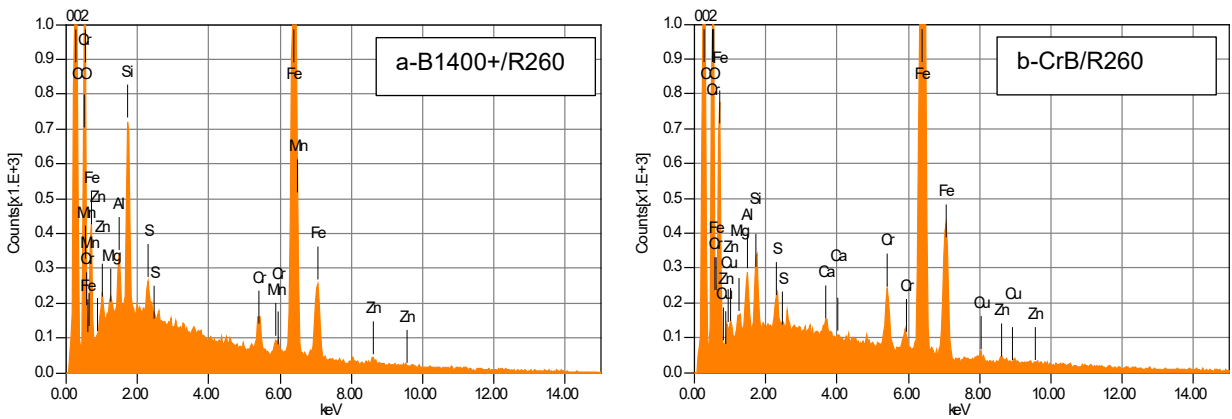


Fig. 15. Comparison of EDS (Energy dispersive spectroscopy) spectrums performed in third body layers, as detailed in Fig.14b and d.

Fig.15 presents the EDS spectrum performed inside the third body layer developed in B1400+ and CrB surfaces. The spectrum shows the presence of metallic elements, for instance Cr and Fe, but also elements that exist exclusively in FM-C suspension such as Al, Mg, Cu and Zn. Moreover, the semi qualitative quantification of elements indicates a high level of oxygen that confirms the presence of oxides in the third body, see table 3.

Table 3 Semi quantitative quantification of the third bodies elements by EDS measurements (% mass).

	C	O	Al	Si	S	Cr	Mn	Cu	Fe
<b>B1400+/R2600</b>	101	28	0.42	1.41	0.18	0.8	0.31	-----	22.34
<b>CrB/R260</b>	83	32	0.48	0.59	0.28	1.36	-----	0.49	37.86

The semi-quantitative evaluation of the third bodies elements in table 3, reveals different compositions. Layers developed in B1400+/R260 interface contain considerable amount of silica, and almost undetectable amount of copper. This confirms the ejection of the large copper particles from the contact area. The copper is not an active element in the development of the third body. Contrary, the layers developed in CrB/R200 interface hold higher copper, and chromium elements. Based on this finding, it seems that the third body developed in B1400+/ R260 induces easier the contacting surface abrasion due the presence of high amount of silica.

Even the CrB surface developed thin third body; it shows the lowest wear volume according to Fig.9. This could be explained by the presence of chromium and copper that reduce the debris detachment. This agrees with the wear surface observed in Fig.16 in both steels. Afterwards, by the influence of the cyclic loading, the mechanical mixing reduces copper particles size, and contributes to the formation of a thin film due to copper ductility. This indicates that the generated layer has a wear protective role.

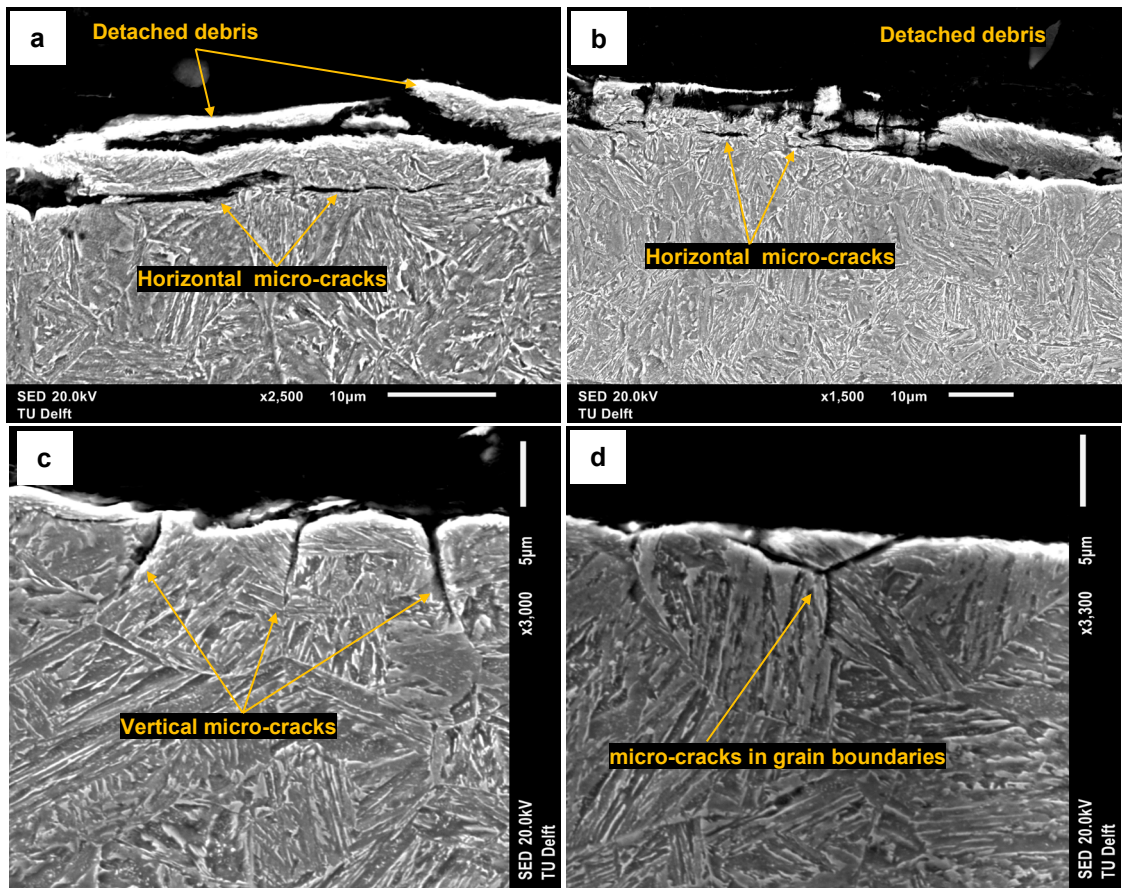


Fig. 16. RCF comparison between B1400+ (a, b) and CrB (c, d) steels after rolling sliding test in presence of FM-C suspension at 0.5% of slip ratio.

Surface scanning of bainitic steels revealed a different behaviour on material pitting process. Fig.16 compares cross-sectioned worn areas between B1400+ and CrB surfaces. It shows that B1400+ is susceptible to horizontal micro-cracks. Contrary, Fig.16 c and d displays micro-cracks developed mainly in the grain boundaries of CrB steel, most of them growth vertically. Both surfaces do not present plastic deformation or slightly visible in detaches debris rather than bainite subsurface.

Concerning FM-S and FM-A suspensions, it would be interesting to investigate further the generation of the protective layers in future by cross-sectioning worn surfaces. Our results using the 2 discs experiment confirm the finding of Oomen et. al.[18]. The reduction of the solid particles size promotes their penetration and dwell inside the contact area. In case of FM-S suspension, silicon and aluminium particles have a complementary hardness and ductility properties leading to an easily mechanical mixing. An excessive contact alimentation would lead to overdoses in the contact by silicon generating an abrasive interlayer (as found by Oomen et. al.[18]). The FM-A suspension contains only metallic solid particles that are copper and aluminium. Mechanical mixing is prompted by the ductile properties of these metals that lead to a very low friction levels. Unrestrained alimentation of FM-A could modify the wear mechanism from an adhesive to a cohesive process.

## 5. Conclusions

Recently developed bainitic steels for railway application were tested using the HOrizontal twin DIsk Machine. The study aims to understand the friction and wear responses under various working conditions; dry contact, in presence of three commercial friction modifiers varying the slip ratio. The relevant results are summarized in the following points:

- After a specific heat treatment, microstructures and properties of recently developed bainitic steels are presented.
- Dry experiments show a stabilized friction in case of the B1400+/R260 system, and a progressive increase of the friction coefficient within CrB/R260 system. Both steels involved abrasive wear indicating a better resistance for CrB/ R260 system compared to B1400+/R260.



- In presence of friction modifiers, the friction evolution had a triangular shape describing the drop of the friction after the suspension application, and a progressive friction increase due to the consumption of the suspension during rolling-sliding. With all tested FMs, it was hard to stabilize the friction coefficient in a window between 0.2 and 0.3. Friction kinetics is untimely related to FMs composition.
- This work shows the formation of a third body on the surface of bainitic steels via SEM observation of cross-sectioned samples.
- The third body generated in the interface of contacting bodies depends on the chemical composition of the FMs, the presence of hard particles could lead to the development of severe abrasive mechanism. The exclusive presence in the FMs composition of ductile metal could cause drastic cohesive wear mechanism.
- RCF response of bainitic steels differs between the promotion of horizontal micro-crack propagation in B1400+ and vertically and grain boundary spreading in CrB steel.

## 6. Acknowledgement

This research has been undertaken within the framework of the Research Program of the Materials innovation institute M2i ([www.m2i.nl](http://www.m2i.nl)) under project number T91.1.12475c. The authors would like to thank the Dutch Rail Infrastructure owner ProRail for their support and Dr. I. Shevtsov for his advices.

## 7. References

- [1] U. Olofsson, Adhesion and friction modification, Woodhead Publishing Limited, 1999. doi:10.1533/9781845696788.1.510.
- [2] R. a Smith, Railways and materials : synergetic progress, 35 (2008) 505–513. doi:10.1179/174328108X318888.
- [3] V.L. Markine, M.J.M.M. Steenbergen, I.Y. Shevtsov, Combatting RCF on switch points by tuning elastic track properties, *Wear*. 271 (2011) 158–167. doi:10.1016/j.wear.2010.10.031.
- [4] L. Deters, M. Proksch, Friction and wear testing of rail and wheel material, *Wear*. 258 (2005) 981–991. doi:10.1016/j.wear.2004.03.045.
- [5] Y. Ma, A.A. Mashal, V.L. Markine, Tribology International Modelling and experimental validation of dynamic impact in 1 : 9 railway crossing panel, *Tribol. Int.* 118 (2018) 208–226. doi:10.1016/j.triboint.2017.09.036.
- [6] R. Stock, R. Pippin, RCF and wear in theory and practice-The influence of rail grade on wear and RCF, *Wear*. 271 (2011) 125–133. doi:10.1016/j.wear.2010.10.015.

- [7] R.I. Carroll, Thesis, Surface Metallurgy and Rolling Contact Fatigue of Rail, Engineering Materials, The University of Sheffield, (2005), <http://etheses.whiterose.ac.uk/14639/>.
- [8] M. Tomicic-Torlakovic, Guidelines for the Rail Grade Selection, *Metalurgija*. 53 (2014) 717–720 <https://hrcak.srce.hr/122230>.
- [9] P.J. Blau, How common is the steady-state? The implications of wear transitions for materials selection and design, *Wear*. 332-333 (2014) 1120–1128. doi:10.1016/j.wear.2014.11.018.
- [10] Y. Zhu, Y. Lyu, U. Olofsson, Mapping the friction between railway wheels and rails focusing on environmental conditions, *Wear*. 324-325 (2015) 122–128. doi:10.1016/j.wear.2014.12.028.
- [11] R. Lewis, U. Olofsson, Mapping rail wear regimes and transitions, *Wear*. 257 (2004) 721–729. doi:10.1016/j.wear.2004.03.019.
- [12] R. Galas, M. Omasta, The Effect of Friction Modifier on the Wheel-Rail Contact, (2016). doi:10.1007/978-3-319-22762-7.
- [13] C. Hardwick, R. Lewis, R. Stock, The effects of friction management materials on rail with pre existing surface damage, 385 (2017) 50–60. doi:10.1016/j.wear.2017.04.016.
- [14] H.K.D.H. Bhadeshia, Novel Steels for Rails, *Encycl. Mater. Sci. Technol.* (2002) 1–7.
- [15] E. Trained, LUBRICANTS FOR RAILWAY TRAFFIC, (n.d.), [www.fuchs-lubritech.com](http://www.fuchs-lubritech.com).
- [16] T.M.H. Lubricants, LUBCON Train , Rail and Wheel Services Tailor Made High-Tech Lubricants for Improved Safety and Reliability LUBCON Train , Rail and Wheel Services From Bow Collector to Break Leverage All from One Source, (n.d.), <http://lubcon.bg/resources/Train-Rail-and-Wheel.pdf>.
- [17] H. Lub, PRODUCT DATA SHEET, (n.d.) 2–3, [http://slovnaft.pl/images/content/LUB\\_repo/A2\\_MSDS\\_MOL%20Polimet%20ME%2018\\_GB.pdf](http://slovnaft.pl/images/content/LUB_repo/A2_MSDS_MOL%20Polimet%20ME%2018_GB.pdf).
- [18] M.A. Oomen, R. Bosman, P.M. Lugt, Characterization of Friction and Wear Behavior of Friction Modifiers used in Wheel-Rail Contacts, (2017) 1–13. <https://www.phmsociety.org/node/2267>
- [19] X. Xu, W. Xu, F. Hipgrave, S. Van Der Zwaag, Design of low hardness abrasion resistant steels, *Wear*. 301 (2013) 89–93. doi:10.1016/j.wear.2013.01.002.
- [20] C. Dayot, A. Saulot, C. Godeau, Y. Berthier, Tribological behaviour of Pearlitic and Bainitic steel grades under various sliding conditions, *Tribol. Int.* 46 (2012) 128–136. doi:10.1016/j.triboint.2011.05.016.